

# Cardiac Magnetic Resonance Imaging for Right Ventricular Disease

MMP Tong<sup>1</sup>, KT Wong<sup>2</sup>

<sup>1</sup>Department of Diagnostic Radiology, Alice Ho Miu Ling Nethersole Hospital, Tai Po, Hong Kong

<sup>2</sup>Department of Imaging and Interventional Radiology, Prince of Wales Hospital, The Chinese University of Hong Kong, Shatin, Hong Kong

## ABSTRACT

Cardiac magnetic resonance is an increasingly popular tool for assessing cardiac anatomy and function, as well as disease pathology, in an objective and comprehensive manner. Establishing diagnosis of diseases involving the right ventricle by traditional transthoracic two-dimensional echocardiography is challenging owing to the peculiar anatomy and retrosternal position of the right ventricle, and chest wall status of the patient. Cardiac magnetic resonance has proven a valuable examination tool in the assessment of the right ventricle in a radiation-free and non-invasive manner. This review describes how cardiac magnetic resonance can nicely depict right ventricle anatomy, morphology, and function, and can aid radiologists and clinicians in assessing diseases involving the right ventricle.

**Key Words:** Heart ventricles; Magnetic resonance imaging

## 中文摘要

### 右心室病的心臟磁共振成像

唐美寶、黃嘉德

心臟磁共振已成為日趨普遍的評估工具，以客觀和全面的角度評估心臟解剖學和功能以及疾病病理學。因為右心室的特殊解剖結構和胸骨後位置以及患者的胸壁狀態，以傳統經胸二維超聲心電圖確診右心室疾病比較困難。事實證明，心臟磁共振能無輻射和非侵入地有效評估右心室狀態。本文綜述心臟磁共振如何恰當描述右心室的解剖結構、形態和功能，幫助放射科醫生和臨床醫生評估涉及右心室的疾病。

**Correspondence:** Dr MMP Tong, Department of Diagnostic Radiology, Alice Ho Miu Ling Nethersole Hospital, Tai Po, Hong Kong. Email: tmp678@ba.org.hk

Submitted: 8 Jun 2018; Accepted: 25 Jun 2018.

Disclosure of Conflicts of Interests: The authors have no conflicts of interest to disclose.

Funding/Support: This research received no specific grant from any funding agency in the public, commercial, or not-for-profit sectors.

## INTRODUCTION

The right ventricle (RV) has been described as a “forgotten chamber” or “neglected side” of the heart; possibly because its role in cardiac physiopathology was previously underestimated.<sup>1,2</sup> Disease involvement of the RV includes congenital structural heart defects, such as tetralogy of Fallot or Ebstein’s anomaly<sup>2</sup>; genetic disorders, such as arrhythmogenic RV cardiomyopathy (ARVC)<sup>3,4</sup>; RV volume overload, such as from intracardiac shunting; and RV pressure overload, such as pulmonary arterial hypertension. Hypertrophic, dilated, and other cardiomyopathies commonly affecting the left ventricle (LV) can also show RV involvement. Common clinical investigative tools for the RV are transthoracic echocardiography and cardiac magnetic resonance (CMR).<sup>1,2,5-9</sup>

Transthoracic echocardiography is more sensitive than CMR in the visualisation and assessment of valves. However, proper RV assessment using transthoracic echocardiography can be difficult, owing to the peculiar anatomy of the RV (thin wall close to epicardial / pericardial fat layer; crescent shape wrapping around the LV; showing no axis of symmetry unlike the LV<sup>10</sup>; presence of trabeculations); the retrosternal position of the RV (which may create acoustic barrier for ultrasound waves); and the individual’s anterior chest wall status (a thick or deformed chest wall can affect ultrasound windowing),<sup>1,2,5-9,11,12</sup> The complex shape of the RV also limits application of geometric models for volume-function measurement.<sup>5</sup>

CMR is a valuable imaging tool in the comprehensive objective assessment of RV anatomy, morphology and function; accurate measurement of volumes and ejection fractions; and characterisation of tissues in a reproducible manner.<sup>1,2,13-15</sup> It is robust, radiation free, and non-invasive.<sup>13</sup> The cardiac structures can be also imaged in different planes thus providing good overview indispensable to diagnosis. Miscellaneous information (such as presence of intra-ventricular thrombus, both qualitative and quantitative assessment of intra-cardiac shunting) can also be nicely depicted using CMR.

Congenital structural heart disease was considered beyond the scope of this article for discussion.

In this review article, we describe the useful CMR sequences essential for RV study and the CMR features of important disease entities involving the RV, with a focus on ARVC and its mimics.

## CARDIAC MAGNETIC RESONANCE IMAGING PROTOCOL

CMR is performed under electrocardiographic gating with an external phased-array surface coil, commonly using a 1.5-T magnetic resonance imaging (MRI) machine. In general, contraindications for MRI also apply to CMR.

Intravenous contrast injection (gadolinium) is unnecessary unless contrast is needed for assessment of intra-ventricular thrombus, viability, and vascular angiogram. Stress study using intravenous adenosine infusion is also unnecessary, unless there is concern of coronary ischaemia that has to be identified.

Cines (function and wall motion assessment) are major features of CMR that require proper breath holding technique of the patient.<sup>14-17</sup> If the patient is unconscious, confused, on a ventilator, or too ill or dyspnoeic, the image quality on cines can be degraded. Severe arrhythmia or ectopics can affect cardiac gating and thus CMR images.<sup>14</sup>

In general, the CMR protocol for RV assessment commonly includes the following steps<sup>17</sup>:

1. Planning scout series of thorax or upper torso. This is a quick, low-resolution scout for planning subsequent acquisition planes.
2. Multi-slice limited thorax anatomy series. These are usually axial studies in dark blood and bright blood sequences that allow for a general overview of both cardiac and extra-cardiac structures. They may include coronal and sagittal planes, which are useful for congenital or structural heart disease assessment.
3. Cines. These are the main series of CMR. Cines use a standard acquisition approach, and different cardiac planes can be obtained. No intravenous contrast is needed. Good image quality can be obtained, if the patient shows adequate breath-holding and no ectopics.
  - Common basic cines include long-axis studies of the LV (Figure 1) and short-axis stacks (Figure 2) for the ventricles. Long-axis LV studies include two-chamber, four-chamber, LV outflow tract view, and its cross-cut.
  - Dedicated cines studies for the RV include: right vertical long axis, which can be thought of as a right-sided two-chamber view (Figure 3); RV outflow tract view (Figure 4) and its cross-cut (Figure 5); RV inflow-outflow tract (Figure 6); and trans-axial stacks of the RV, which image the entire RV chamber from cranial to



**Figure 1.** Routine long-axis cines of left ventricle: two-chamber study (2CH); four-chamber study (4CH); left ventricular outflow tract study (LVOT); and left ventricular outflow tract cross-cut study (LVOT XC).



**Figure 2.** Routine short-axis cines at basal, mid-ventricular, and apical levels. Short-axis cine stacks are obtained via positioning planes in the four-chamber and two-chamber studies by aligning consecutive planes perpendicular to the long axis of left ventricle from the atrioventricular groove towards the apex, with interslice gaps. Short-axis cine stacks are essential for assessment of volume and ejection fractions of both left ventricle and right ventricle.

caudal directions in a contiguous axial manner by positioning axial planes in the thorax study (Figure 7). Dedicated RV cines are important

because common basic cines studies may not be adequate for assessing the entire RV, owing to its peculiar anatomy.

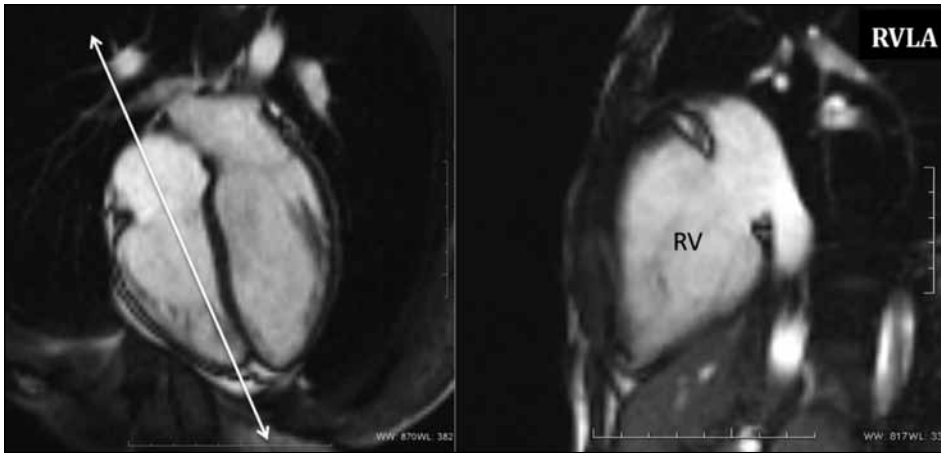


**Figure 3.** The right vertical long-axis (RVLA) cine is obtained via the four-chamber cine by acquiring a plane positioned through the right atrium, tricuspid valve, and right ventricle (RV), as well as aligning parallel to the inter-ventricular septum.

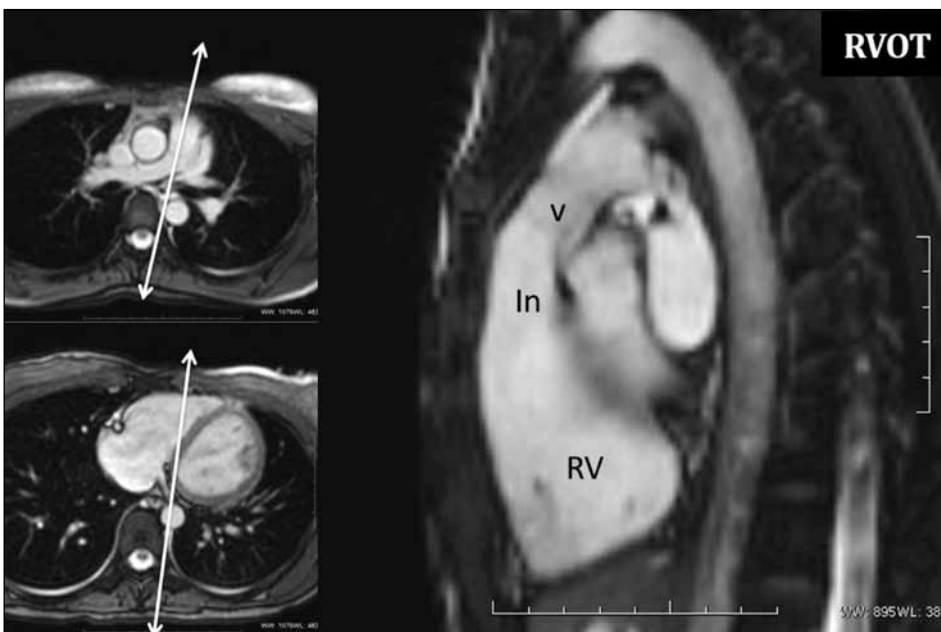


**Figure 4.** The right ventricular outflow tract (RVOT) cine is obtained via the initial multi-slice limited thorax anatomical study, by positioning a plane through the pulmonary trunk and the RV lumen.

Abbreviations: In = pulmonary infundibulum; RV = right ventricle; v = pulmonary valve.

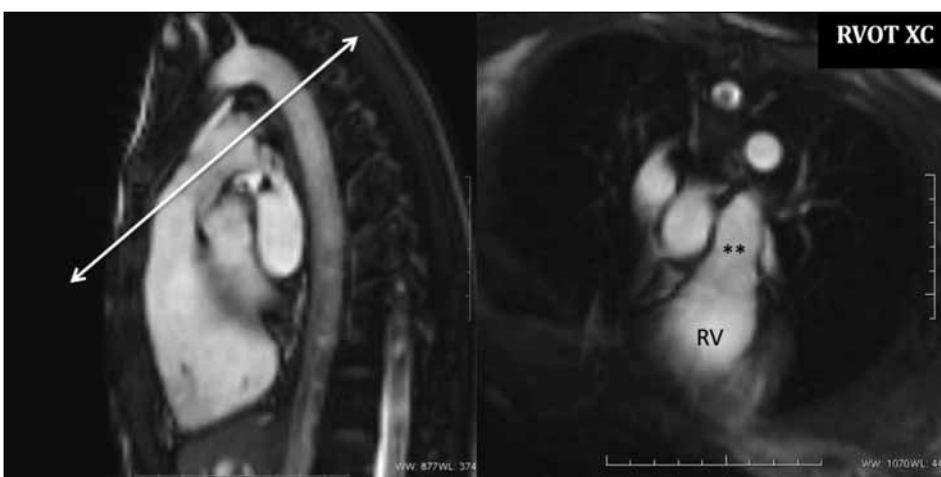


**Figure 5.** The right ventricular outflow tract (RVOT) cross-cut (XC) cine is obtained by positioning a plane perpendicular to the RVOT. The proximal part of the pulmonary outflow tract is also shown (asterisks).

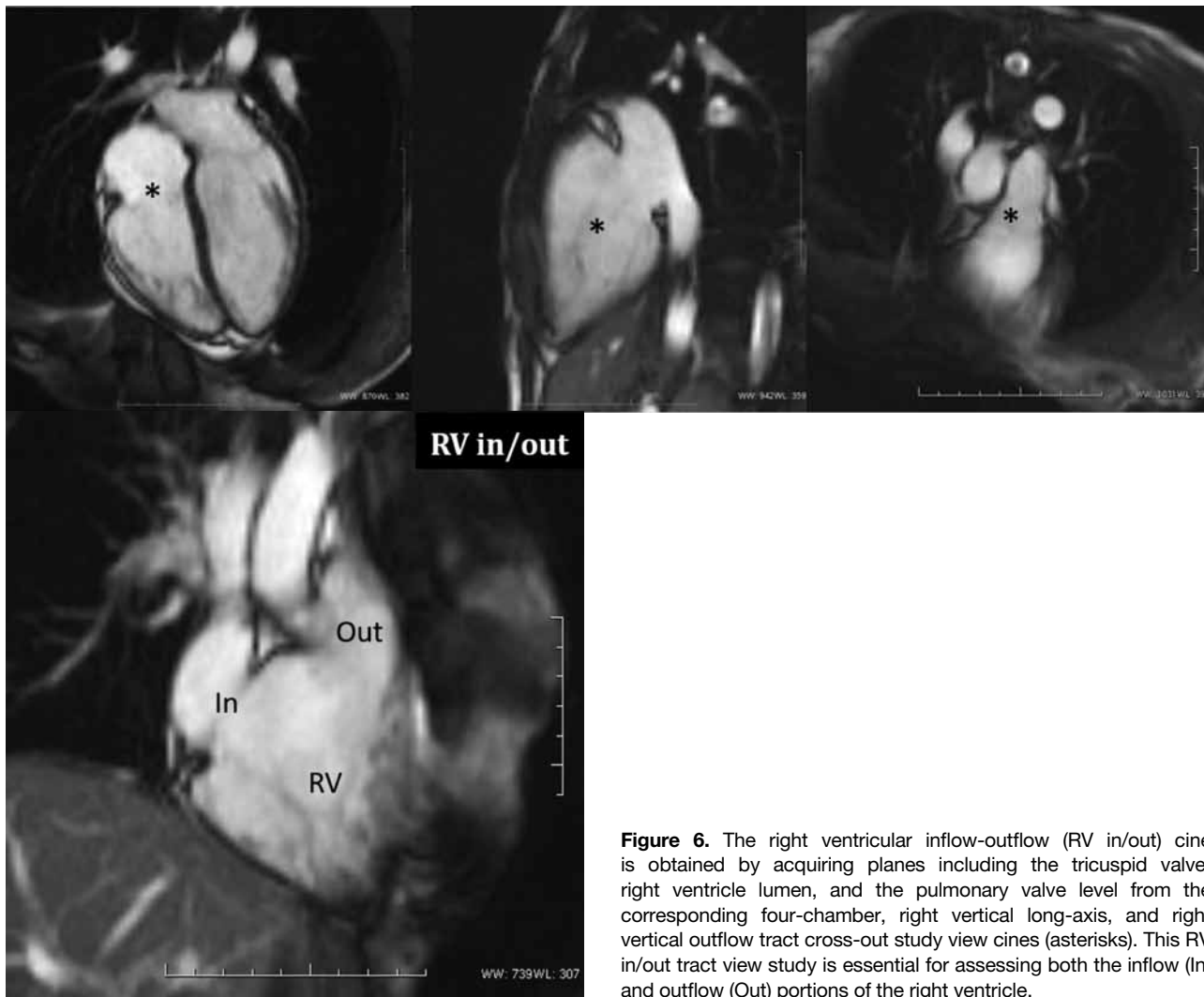


**Figure 6.** The right ventricular inflow-outflow (RV in/out) cine is obtained by acquiring planes including the tricuspid valve, right ventricle lumen, and the pulmonary valve level from the corresponding four-chamber, right vertical long-axis, and right vertical outflow tract cross-out study view cines (asterisks). This RV in/out tract view study is essential for assessing both the inflow (In) and outflow (Out) portions of the right ventricle.

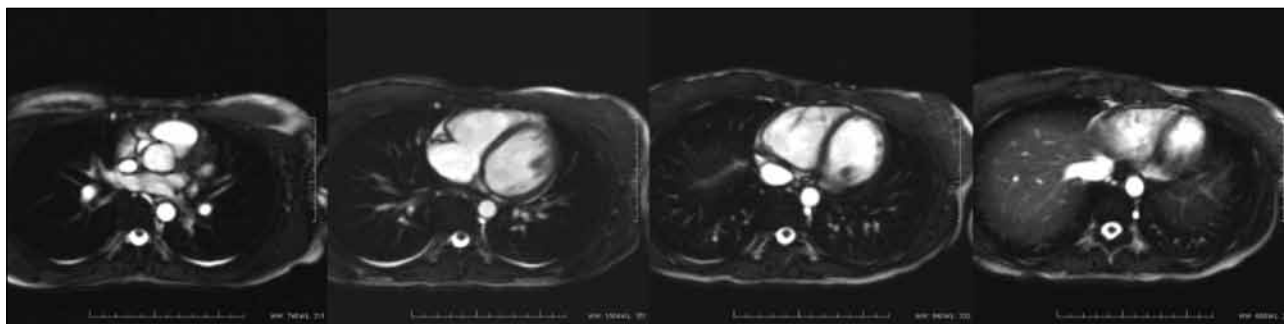


**Figure 7.** Cine stacks of the right ventricle are obtained by acquiring consecutive axial cines of the thorax, including entire right ventricle coverage from cranial to caudal direction (only selected axial levels are shown here).

4. Optional sequences. These include: early gadolinium study for detection of intra-ventricular thrombus, which is useful in dilated ventricular chambers; late gadolinium study, which is useful for viability

and myocardial wall fibrosis assessment; flow velocity study, which is useful for qualitative and quantitative assessment of intra-cardiac shunting; and vascular angiogram, which is useful for detection

of extracardiac shunt.

Routine short-axis cine studies of the LV already include RV coverage, allowing for volume and ejection fraction assessment for both the LV and the RV, using semi-automated software. Assessment of intra-cardiac shunt can be done either indirectly or directly.<sup>17</sup> Indirect assessment is done via flow measurement across both RV and LV outflow tracts using the phase contrast technique, under standard planes and proper velocity encoding, with calculation of the Qp:Qs ratio (shunt ratio between pulmonary and systemic circulations). A Qp:Qs ratio >2.0 indicates significant intracardiac shunting. Direct assessment is done via en-face imaging directly over the visualised shunt defect (such as the atrial septal defect).

### ARRHYTHMOGENIC RIGHT VENTRICULAR CARDIOMYOPATHY

ARVC (also known as arrhythmogenic RV dysplasia) is an inherited genetic disease that affects the RV. It is autosomal dominant with variable penetrance and disease expression. The disease is characterised by pathological fibrofatty replacement of RV myocardium.<sup>3,4,18,19</sup> The prevalence of ARVC is 1:1000-5000 with male predominance. The age at symptom onset ranges from age 20 to 40 years. Clinical symptoms of ARVC are non-specific and can include palpitations and light-headedness.<sup>18</sup> ARVC can exhibit LV involvement or, in advanced stages, bi-ventricular involvement. ARVC is one of the leading cause of sudden cardiac death in young people or athletes due to fatal arrhythmia.

Disease expression of ARVC is variable, from the 'clinically concealed phase' (asymptomatic, at risk of sudden cardiac death if acute exertion), through the 'overt electrical phase' (symptomatic arrhythmia), to cardiac failure.<sup>3</sup>

The common area of involvement is the 'triangle of dysplasia' (bounded by the inflow tract, the outflow tract, and the RV apex),<sup>3</sup> which can be assessed in the dedicated cines for the RV (in particular the RV inflow-outflow tract; RV outflow tract, and RV outflow tract cross-cut series). Global RV involvement is possible.

Motion abnormalities (focal akinesia, dyskinesia or dyssynchronous motion); impaired RV ejection fraction and elevated end-diastolic RV volume indexed to patient's body surface area are seen in ARVC. There are specific diagnostic criteria of ARVC from cardiac MRI as suggested in the revised task force criteria, which are useful for radiologists and clinicians to follow (Table).<sup>3</sup> The CMR features of a histologically proven case of ARVC (from cardiac transplant) are illustrated in Figures 8 to 13.

Identification of ARVC is important as early clinical attention or management can ensue. In selected patients, prophylactic implantable cardioverter defibrillator is indicated.<sup>18</sup> The imaging diagnosis of ARVC is based on the revised task force criteria.<sup>3,4</sup> In the revised task force criteria,<sup>3</sup> the imaging part relies on two-dimensional echocardiography or CMR. The revised task force criteria are more specific and objective with definition on RV volumes and ejection fraction (Table).<sup>3</sup>

In the revised task force criteria, there is no need for depiction of abnormal fibrofatty infiltration to establish the diagnosis of ARVC on MRI.<sup>3</sup> In fact, demonstration of abnormal fibrofatty infiltration on CMR is difficult,<sup>19</sup> owing to the thin RV wall and normal presence of an epicardial / pericardial fat layer. Also, intramyocardial and epicardial fat can increase with body weight and age but the prevalence is unknown (Figure 14).<sup>19</sup> Therefore, the recommended CMR protocol does not include fat suppression study.

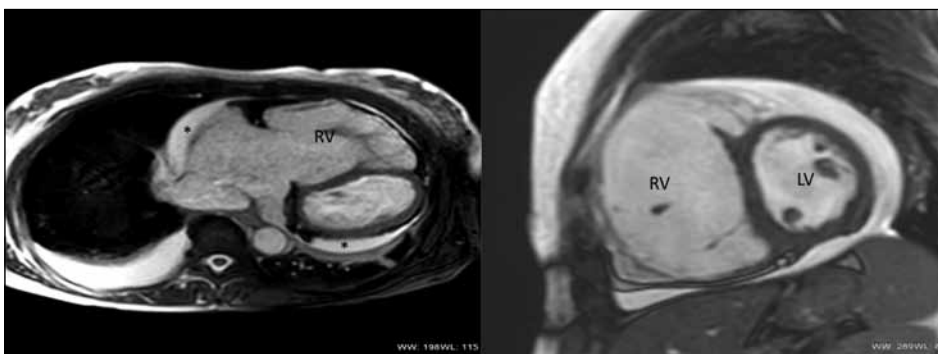


**Figure 8.** Axial slice of a multi-slice bright blood thorax study (left) showing dilated right ventricle (RV), presence of pericardial effusion (asterisks) and right basal pleural effusion. Short-axis study (right) taken at the mid-ventricular level in end-diastole showing left ventricle (LV), dilated RV lumen, and D-shaped septum indicating right ventricular volume overload.

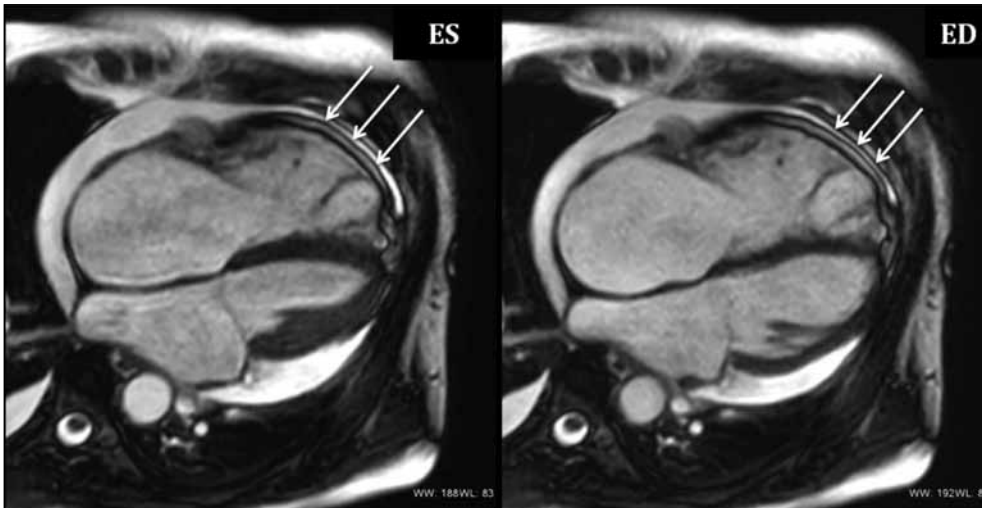


**Figure 9.** Four-chamber study in end-systole (ES) and end-diastole (ED) phases demonstrates akinesia in the right ventricular free wall (arrows). There is not much difference between the right ventricular volumes at end-systole and end-diastole phases, indicating severe impaired right ventricular ejection fraction. Note the D-shaped septum at end-diastole (not observed in end-systole), indicating right ventricular volume overload.

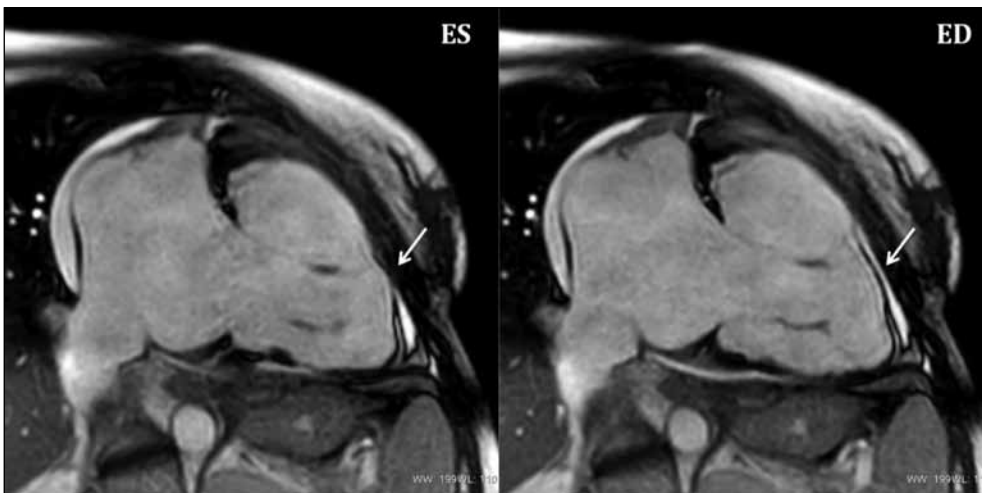


**Figure 10.** Right vertical long-axis study in end-systole (ES) and end-diastole (ED) phases demonstrates focal dyskinesia in part of the right ventricle free wall (arrows). There is not much difference between the right ventricular volumes at end-systole and end-diastole phases, indicating severe impaired right ventricular ejection fraction.

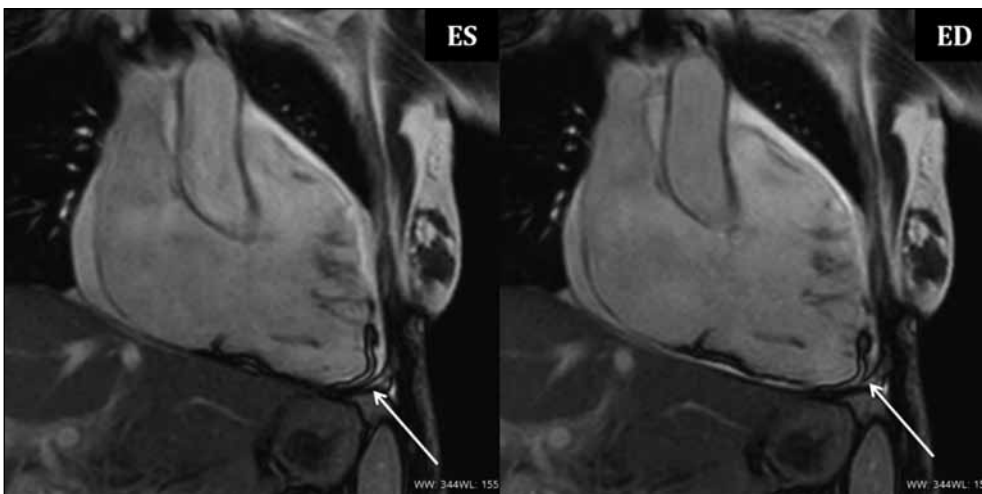


**Figure 11.** Cine study of right ventricular inflow-outflow tract showing akinesia in the right ventricular apex (arrows) at end-systole (ES) and end-diastole (ED) phases.

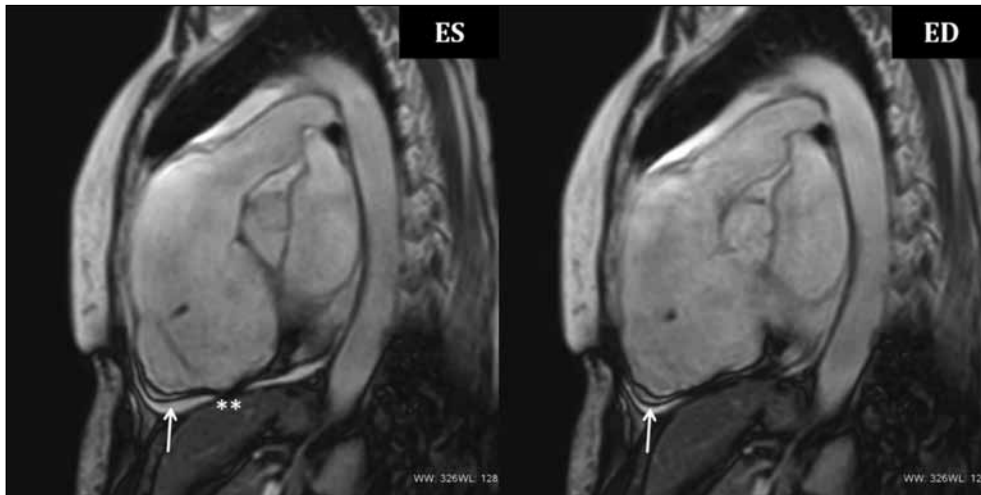


**Figure 12.** Right ventricular outflow tract in end-systole (ES) and end-diastole (ED) phases demonstrates akinesia in the right ventricle apex (arrows), and focal dyskinesia in the right ventricular inferior wall (asterisks).

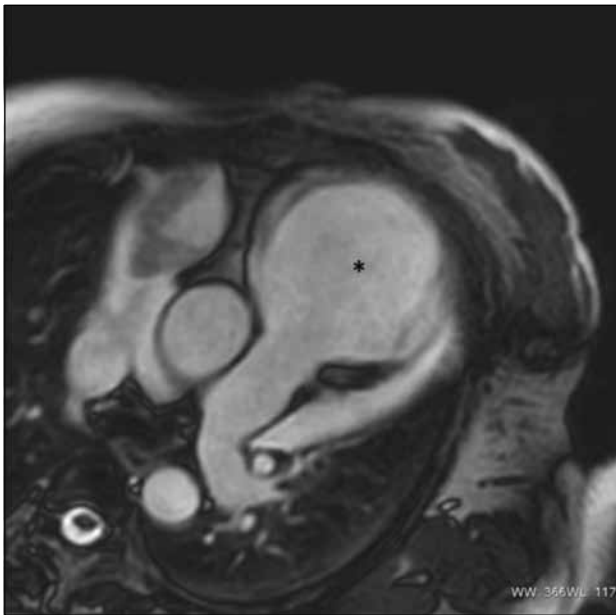


**Figure 13.** Right ventricular outflow tract cross-cut study cine showing dilated right ventricular outflow tract (asterisk).

### MIMICS OF ARRHYTHMOGENIC RIGHT VENTRICULAR CARDIOMYOPATHY

Mimics of ARVC on MRI include diseases causing dilated RV chamber or increased RV volumes (including RV volume overload from intra-cardiac shunting, such as with atrial septal defect, anomalous pulmonary vascular return, or severe tricuspid regurgitation), or apparent deformed RV chamber (eg, partial agenesis of pericardium).<sup>22</sup>

In general, mimics of ARVC can be distinguished from routine CMR sequences. In some patients, flow-velocity study across the RV outflow tract (Qp) and ascending aorta (Qs) is recommended for assessment of any significant intracardiac shunt. The measured Qp:Qs ratio is an indirect assessment of intracardiac shunt (Figures 15-18). Direct assessment of shunt can be immediately directed over the shunt defect.

Identification of significant intracardiac shunt is essential, as a false label of ARVC can result in a great difference in clinical management and can also lead to undue patient anxiety owing to unnecessary family screening.

### Pressure-overload of Right Ventricle

Pressure overload of the RV can result from pulmonary hypertension or other miscellaneous conditions.<sup>22</sup> This can be manifested on CMR as RV hypertrophy and presence of abnormal septal bouncing (D-shaped septum in both systole and diastole). A rare case of large vessel vasculitis affecting the pulmonary trunk, main pulmonary arteries, and ascending aorta causing RV hypertrophy is shown in Figures 19 to 21.

Review on literature comparing the original and revised task force criteria reveals an intermediate subgroup that previously fell into previous criteria, but are not entirely accounted for in the revised 2010 task force criteria.<sup>20,21</sup> There may be clinical challenges related to this intermediate subgroup. Some authors suggest further review as to the proper follow-up or management plan for this subgroup.<sup>20,21</sup>

**Table.** Comparison of original and revised task force criteria<sup>3</sup>

Original task force criteria	Revised task force criteria
Global or regional dysfunction and structural alterations	
Major	
<ul style="list-style-type: none"> <li>• Severe dilatation and reduction of right ventricular ejection fraction with no (or only mild) left ventricular impairment</li> <li>• Localised right ventricular aneurysms (akinetic or dyskinetic areas with diastolic bulging)</li> <li>• Severe segmental dilatation of the right ventricle</li> </ul>	<p>By two-dimensional echocardiography</p> <ul style="list-style-type: none"> <li>• Regional right ventricular akinesia, dyskinesia, or aneurysm; and</li> <li>• One of the following (end diastole):                             <ul style="list-style-type: none"> <li>o Parasternal long-axis view right ventricular outflow tract <math>\geq 32</math> mm (corrected for body size [parasternal long axis / body surface area] <math>\geq 19</math> mm/m<sup>2</sup>)</li> <li>o Parasternal short-axis right ventricular outflow tract <math>\geq 36</math> mm (corrected for body size [parasternal short axis/body surface area] <math>\geq 21</math> mm/m<sup>2</sup>)</li> <li>o Fractional area change <math>\leq 33\%</math></li> </ul> </li> </ul> <p>By magnetic resonance imaging</p> <ul style="list-style-type: none"> <li>• Regional right ventricular akinesia or dyskinesia or dyssynchronous right ventricular contraction; and</li> <li>• One of the following:                             <ul style="list-style-type: none"> <li>o Ratio of right ventricular end-diastolic volume to body surface area <math>\geq 110</math> mL/m<sup>2</sup> (male) or <math>\geq 100</math> mL/m<sup>2</sup> (female)</li> <li>o Right ventricular ejection fraction <math>\leq 40\%</math></li> </ul> </li> </ul> <p>By right ventricular angiography</p> <ul style="list-style-type: none"> <li>• Regional right ventricular akinesia, dyskinesia, or aneurysm</li> </ul>
Minor	
<ul style="list-style-type: none"> <li>• Mild global right ventricular dilatation and/or ejection fraction reduction with normal left ventricle</li> <li>• Mild segmental dilatation of the right ventricle</li> <li>• Regional right ventricular hypokinesia</li> </ul>	<p>By two-dimensional echocardiography</p> <ul style="list-style-type: none"> <li>• Regional right ventricular akinesia or dyskinesia; and</li> <li>• One of the following (end diastole):                             <ul style="list-style-type: none"> <li>o Parasternal long-axis view right ventricular outflow tract <math>\geq 29</math> to <math>&lt; 32</math> mm (corrected for body size [parasternal long-axis/body surface area] <math>\geq 16</math> to <math>&lt; 19</math> mm/m<sup>2</sup>)</li> <li>o Parasternal short-axis right ventricular outflow tract <math>\geq 32</math> to <math>&lt; 36</math> mm (corrected for body size [parasternal short axis/body surface area] <math>\geq 18</math> to <math>&lt; 21</math> mm/m<sup>2</sup>)</li> <li>o Fractional area change <math>&gt; 33\%</math> to <math>\leq 40\%</math></li> </ul> </li> </ul> <p>By magnetic resonance imaging</p> <ul style="list-style-type: none"> <li>• Regional right ventricular akinesia or dyskinesia or dyssynchronous right ventricular contraction; and</li> <li>• One of the following:                             <ul style="list-style-type: none"> <li>o Ratio of right ventricular end-diastolic volume to body surface area <math>\geq 100</math> to <math>&lt; 110</math> mL/m<sup>2</sup> (male) or <math>\geq 90</math> to <math>&lt; 100</math> mL/m<sup>2</sup> (female)</li> <li>o Right ventricular ejection fraction <math>&gt; 40\%</math> to <math>\leq 45\%</math></li> </ul> </li> </ul>



**Figure 14.** Axial computed tomography study showing presence of fat in right ventricular free wall and right ventricular outflow tract (arrows). This is non-specific and can be seen in some otherwise healthy older individuals.

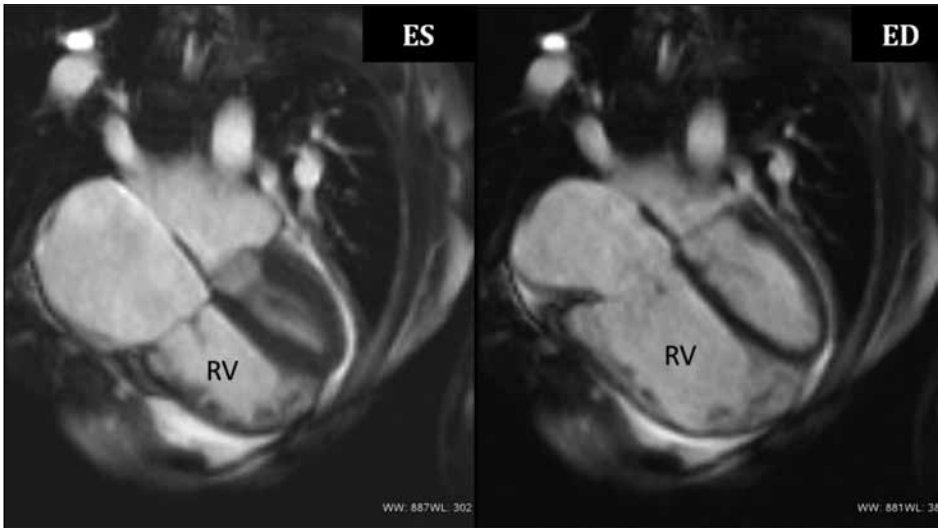


**Figure 15.** Four-chamber study in end-systole (ES) and end-diastole (ED) phases showing dilated right ventricle (RV). No evidence of associated D-shaped septum is visible in this patient.



**Figure 16.** Captured short-axis cine study in mid-ventricular level showing dilated right ventricle (RV).

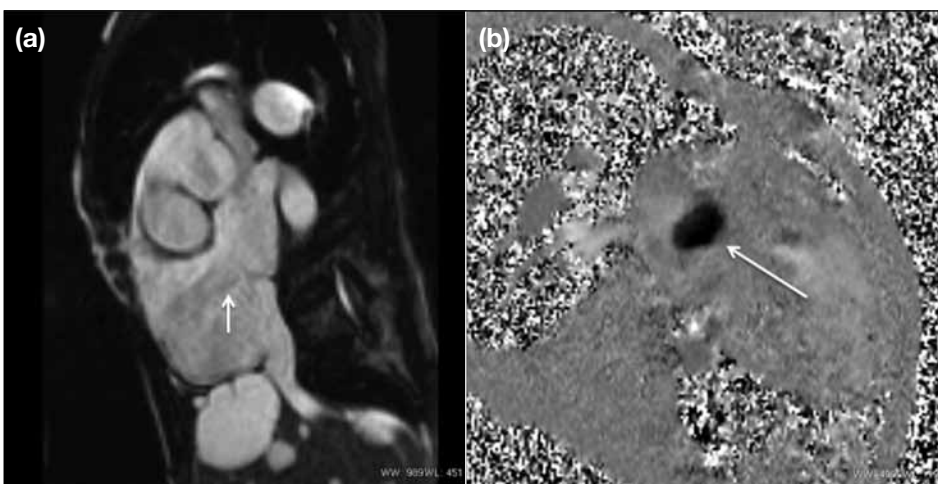


**Figure 17.** (a) Captured cine showing presence of an atrial septal defect jet (arrow). (b) Flow velocity study showing presence of atrial septal defect (arrow) imaged in plane view.

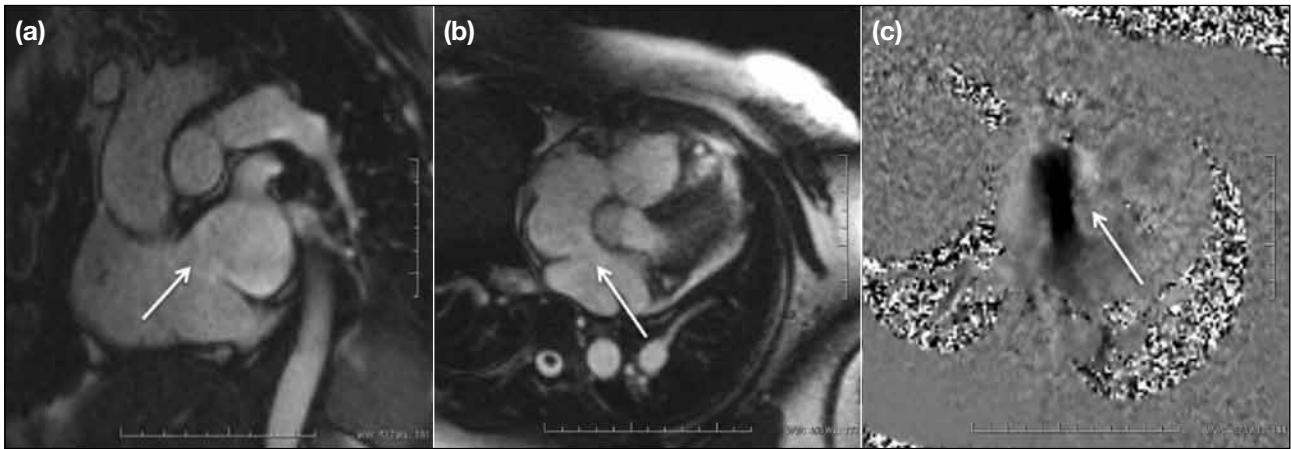


**Figure 18.** (a and b) Captured cine shots showing the atrial septal defect (ASD) jet enface both through-plane and in-plane respectively (arrows). (c) Flow velocity study of the ASD jet.

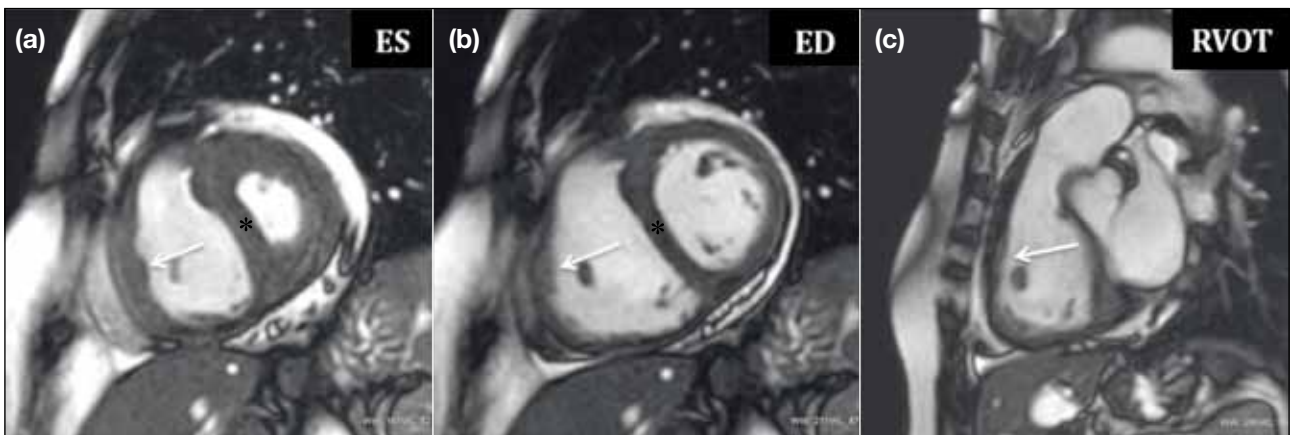


**Figure 19.** Short-axis study taken at mid-ventricular level showing evidence of right ventricular pressure overload with right ventricular hypertrophy (arrows), presence of D-shaped septum (asterisks) at (a) end-systole (ES) and (b) end-diastole (ED). (c) The right ventricular outflow tract (RVOT) view displays right ventricular hypertrophy (arrow). Normal right ventricular wall thickness is thin; wall thickness more than 4-5 mm in end-diastole indicates right ventricular hypertrophy.

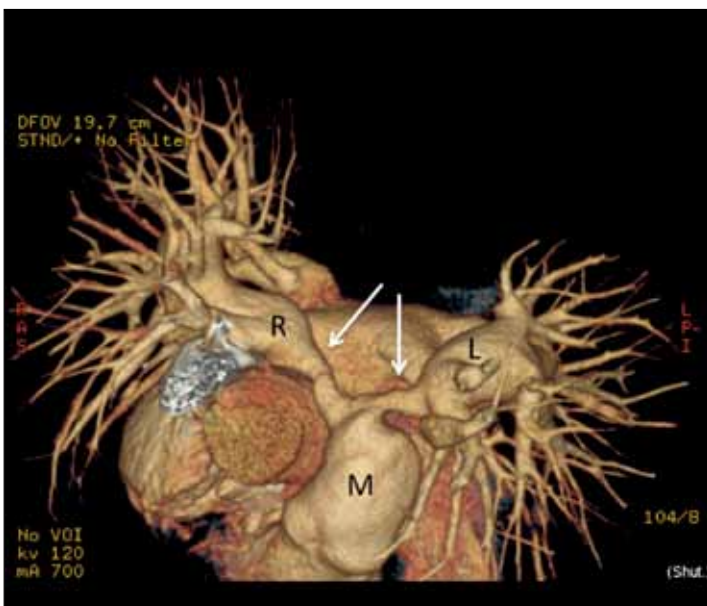


**Figure 20.** Computed tomography study in volume rendering reformat showing marked stenoses in both main right and left pulmonary arteries (arrows) associated with post-stenotic dilations. This is causing right ventricular hypertrophy.

Abbreviations: M = main pulmonary trunk; R = right main pulmonary artery; L = left main pulmonary artery).

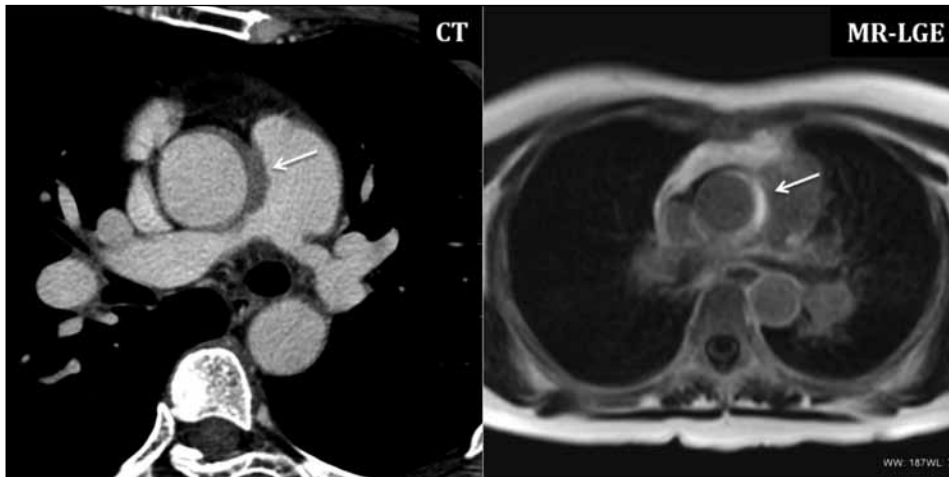


**Figure 21.** Axial computed tomography (CT) image and magnetic resonance late gadolinium enhancement (MR-LGE) study showing focal eccentric wall thickening in the proximal ascending aorta and presence of late enhancement on MR imaging indicating prior aortic wall inflammation or fibrosis; which might be observed in large vessel vasculitis. This is a rare cause of right ventricular pressure overload.

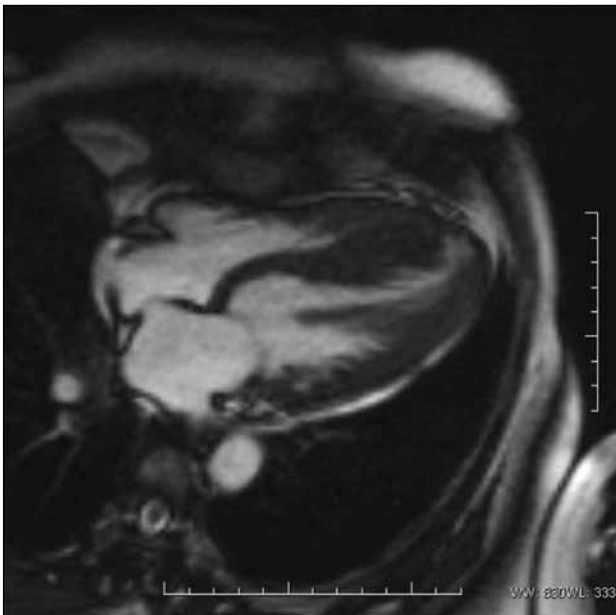


**Figure 22.** Hypertrophic cardiomyopathy involving both ventricles.

### Other Diseases Affecting the Right Ventricle

Common disease entities affecting the LV may display RV involvement, such as hypertrophic or dilated cardiomyopathies (Figure 22).

### CONCLUSION

The RV can be difficult to depict on clinical grounds and on transthoracic two-dimensional echocardiography. CMR is a promising imaging tool in the assessment of RV anatomy and function, as well as disease pathology,

in a comprehensive and objective manner. It is also radiation free and non-invasive. CMR sequences can aid radiologists and clinicians in the proper assessment of diseases involving the RV.

### REFERENCES

1. Galea N, Carbone I, Cannata D, Cannavale G, Conti B, Galea R, et al. Right ventricular cardiovascular magnetic resonance imaging: normal anatomy and spectrum of pathological findings. *Insights Imaging*. 2013;4:213-23. [Crossref](#)
2. Valsangiacomo Buechel E, Mertens LL. Imaging the right ventricle: the use of integrated multimodality imaging. *Eur Heart J*. 2012;33:949-60. [Crossref](#)
3. Marcus FI, McKenna WJ, Sherrill D, Basso C, Bauce B, Bluemke DA, et al. Diagnosis of arrhythmogenic right ventricular cardiomyopathy/dysplasia: proposed modification of the task force criteria. *Circulation*. 2010;121:1533-41. [Crossref](#)
4. te Riele AS, Tandri H, Bluemke DA. Arrhythmogenic right ventricular cardiomyopathy (ARVC): cardiovascular magnetic resonance update. *J Cardiovasc Magn Reson*. 2014;16:50. [Crossref](#)
5. Sanz J, Conroy J, Narula J. Imaging of the right ventricle. *Cardiol Clin*. 2012;30:189-203. [Crossref](#)
6. Lindqvist P, Calcuttea A, Henein M. Echocardiography in the assessment of right heart function. *Eur J Echocardiogr*. 2008;9:225-34.
7. Karas MG, Kizer JR. Echocardiographic assessment of the right ventricle and associated hemodynamics. *Prog Cardiovasc Dis*. 2012;55:144-60. [Crossref](#)
8. Markley RR, Ali A, Potfay J, Paulsen W, Jovin IS. Echocardiographic evaluation of the right heart. *J Cardiovasc Ultrasound*. 2016;24:183-90. [Crossref](#)
9. Rudski LG, Lai WW, Afilalo J, Hua L, Handschumacher MD, Chandrasekaran K, et al. Guidelines for the echocardiographic assessment of the right heart in adults: a report from the American Society of Echocardiography endorsed by the European Association of Echocardiography, a registered branch of the European Society of Cardiology, and the Canadian Society of Echocardiography. *J Am Soc Echocardiogr* 2010;23:685-713. [Crossref](#)
10. Capelastegui Alber A, Astigarraga Aguirre E, de Paz MA, Larena Iturbe JA, Salinas Yeregui T. Study of the right ventricle using

- magnetic resonance imaging [in Spanish]. *Radiologia*. 2012;54:231-45. [Crossref](#)
11. Dell'Italia LJ. Anatomy and physiology of the right ventricle. *Cardiol Clin*. 2012;30:167-87. [Crossref](#)
  12. Fairbairn TA, Motwani M, Greenwood JP, Plein S. CMR for the diagnosis of right heart disease. *JACC Cardiovasc Imaging*. 2012;5:227-9. [Crossref](#)
  13. Parsai C, O'Hanlon R, Prasad SK, Mohiaddin RH. Diagnostic and prognostic value of cardiovascular magnetic resonance in non-ischaemic cardiomyopathies. *J Cardiovasc Magn Reson*. 2012;14:54. [Crossref](#)
  14. Leung S. Right ventricular ejection fraction. Available from: <https://scmr.org/page/RVEF?>. Accessed 1 Nov 2017.
  15. Hussain T. Arrhythmogenic right ventricular cardiomyopathy/dysplasia (ARVC/D). Available from: <https://scmr.org/page/ARVC-D?&hhsearchterms=%22arrhythmogenic+and+right+and+ventricular+and+cardiomyopathy%2fdy%22>. Accessed 1 Nov 2017.
  16. Ginat DT, Fong MW, Tuttle DJ, Hobbs SK, Vyas RC. Cardiac imaging: Part 1, MR pulse sequences, imaging planes, and basic anatomy. *AJR Am J Roentgenol*. 2011;197:808-15. [Crossref](#)
  17. Myerson SG, Francis J, Neubauer S. *Cardiovascular Magnetic Resonance*. Oxford: Oxford University Press; 2010. [Crossref](#)
  18. Castaños Gutiérrez SL, Kamel IR, Zimmerman SL. Current concepts on diagnosis and prognosis of arrhythmogenic right ventricular cardiomyopathy/dysplasia. *J Thoracic Imaging*. 2016;31:324-35. [Crossref](#)
  19. Ramen SV, Basso C, Tandri H, Taylor MR. Imaging phenotype vs genotype in nonhypertrophic heritable cardiomyopathies: dilated cardiomyopathy and arrhythmogenic right ventricular cardiomyopathy. *Circ Cardiovascular Imaging*. 2010;3:753-65. [Crossref](#)
  20. Vermes E, Strohm O, Otmani A, Childs H, Duff H, Friedrich MG. Impact of the revision of arrhythmogenic right ventricular cardiomyopathy/dysplasia task force criteria on its prevalence by CMR criteria. *JACC Cardiovascular Imaging*. 2011;4:282-7. [Crossref](#)
  21. Femia G, Hsu C, Singarayar S, Sy RW, Kilborn M, Parker G, et al. Impact of new task force criteria in the diagnosis of arrhythmogenic right ventricular cardiomyopathy. *Int J Cardiol*. 2014;171:179-83. [Crossref](#)
  22. Quarta G, Husain SI, Flett AS, Sado DM, Chao CY, Tomé Esteban MT, et al. Arrhythmogenic right ventricular cardiomyopathy mimics: role of cardiovascular magnetic resonance. *J Cardiovasc Magn Reson*. 2013;15:16. [Crossref](#)